Original Article

A bioengineered in situ ovary (ISO) supports follicle engraftment and live-births post-chemotherapy

Journal of Tissue Engineering
Volume 14: 1–18

DOI: 10.1177/20417314231197282
journals.sagepub.com/home/tej
Sage

Michael J Buckenmeyer[1,2,3], Meena Sukhwani[4], Aimon Iftikhar[1,2], Alexis L Nolfi[1,2], Ziyu Xian[1], Srujan Dadi[1], Zachary W Case[2], Sarah R Steimer[4], Antonio D'Amore[2,5], Kyle E Orwig[4] and Bryan N Brown[1,2,4]

Abstract

Female cancer patients who have undergone chemotherapy have an elevated risk of developing ovarian dysfunction and failure. Experimental approaches to treat iatrogenic infertility are evolving rapidly; however, challenges and risks remain that hinder clinical translation. Biomaterials have improved in vitro follicle maturation and in vivo transplantation in mice, but there has only been marginal success for early-stage human follicles. Here, we developed methods to obtain an ovarian-specific extracellular matrix hydrogel to facilitate follicle delivery and establish an in situ ovary (ISO), which offers a permissive environment to enhance follicle survival. We demonstrate sustainable follicle engraftment, natural pregnancy, and the birth of healthy pups after intraovarian microinjection of isolated exogenous follicles into chemotherapy-treated (CTx) mice. Our results confirm that hydrogel-based follicle microinjection could offer a minimally invasive delivery platform to enhance follicle integration for patients post-chemotherapy.

Keywords

Biomaterials, tissue engineering, decellularization, extracellular matrix hydrogels, fertility preservation

Date received: 3 May 2023; accepted: 10 August 2023

Introduction

Ovarian follicles are the major functional component of the ovary that produce hormones (e.g. estrogen) and mature eggs for ovulation.[1,2] Chemotherapy, radiation, and other physical or chemical insults can damage or deplete the ovarian follicle pool, resulting in premature ovarian insufficiency (POI), compromising ovarian hormone production and fecundity.[3–5] Ovarian tissue cryopreservation is the primary option used to preserve the fertility of patients who cannot afford to delay gonadotoxic treatment long enough for ovarian stimulation and cryopreservation of oocytes. Upon remission, the ovarian cortex, which is rich in primordial follicles, can be transplanted back into patient survivors to establish natural pregnancies or undergo in vitro fertilization (IVF).[6–14] While ovarian tissue transplantation is widely considered to be minimally invasive, it remains a major surgical procedure and may

[1]Department of Bioengineering, University of Pittsburgh, Pittsburgh, PA, USA
[2]McGowan Institute for Regenerative Medicine, University of Pittsburgh, Pittsburgh, PA, USA
[3]Cancer Innovation Laboratory, Center for Cancer Research, National Cancer Institute, National Institutes of Health, Frederick, MD, USA
[4]Department of Obstetrics, Gynecology and Reproductive Sciences, Magee-Womens Research Institute, University of Pittsburgh School of Medicine, Pittsburgh, PA, USA
[5]Fondazione RiMED, Palermo, Italy

Corresponding authors:
Bryan N Brown, Department of Bioengineering, University of Pittsburgh, 450 Technology Drive, Suite 300 BSPII, Pittsburgh, PA 15219, USA.
Email: brownb@upmc.edu

Kyle E Orwig, Department of Obstetrics, Gynecology and Reproductive Sciences, Magee-Womens Research Institute, University of Pittsburgh School of Medicine, 204 Craft Avenue, Pittsburgh, PA 15213, USA.
Email: orwigke@upmc.edu

not be appropriate in cases where the ovarian tissues may harbor malignant cells (e.g. leukemia). To address these issues, other experimental alternatives, such as in vitro follicle maturation (IVM) and artificial ovaries, use isolated immature follicles from the stroma to reduce the potential for co-transplantation of cancer cells. These methods have been used to achieve complete folliculogenesis and have led to live-births in mouse models of infertility, but several challenges must be addressed prior to their clinical translation for human patients.

A major obstacle for restoring reproductive function and fertility has been the inability to accurately mimic the dynamic environment of the human ovary. In healthy post-pubertal women, ovarian follicles can exist at multiple stages of development within various regions of the ovary, while preferentially and simultaneously responding to endocrine, paracrine and autocrine signals that coordinate their maturation. For example, quiescent primordial follicles reside in the stiff outer cortex, and as they are activated into the growing pool, pre-antral and antral follicles migrate toward the medulla, which is a more compliant environment for exponential growth. While our understanding of the spatiotemporal, biochemical, and mechanical signaling cues is improving, it remains poorly defined. A potential solution may be to use the ovary as a transplantation site for isolated immature follicles. Intraovarian transplantation has successfully generated live-births from infertile mice after the delivery of female germline stem cells.[15–17] However, the existence and characterization of ovarian stem cells in the human adult ovary remains controversial.[18,19] Alternatively, intraovarian transplantation of isolated primordial follicles may have the potential to replenish the ovarian reserve of cancer patients post-chemotherapy. A previous attempt to restore fertility after chemotherapy using this approach resulted in follicle apoptosis.[20] Based upon these findings, we hypothesized that immature follicles may benefit from the additional support of a biomaterial that facilitates integration within the ovary and promotes long-term survival and function.

One option to improve the effectiveness of intraovarian follicle transplantation, integration, and survival is the use of a tissue-specific extracellular matrix (ECM) hydrogel. ECM hydrogels have been used to treat a spectrum of diseases due to their intrinsic ability to promote tissue remodeling.[21,22] To obtain ECM hydrogels, tissues must first be decellularized to remove immunogenic components. The process of decellularization can be used to preserve an ovarian-specific acellular scaffold, which is composed of a unique profile of ECM proteins, proteoglycans, glycoproteins, and sequestered biomolecules (e.g. growth factors).[23,24] Recently, bovine ovaries were decellularized using sodium dodecyl sulfate (SDS) to obtain a tissue-specific scaffold, which was re-seeded with healthy follicles and transplanted to restore cycling in an ovariectomized mouse.[25] Similarly, porcine and bovine ovaries were decellularized then processed into ECM composite "tissue papers," demonstrating a versatile approach for short-term in vitro culture of nonhuman primate and human ovarian cortical strips.[26] Other research has cited the use of SDS to decellularize human ovarian medulla and cortical tissues but observed low follicle recovery rates upon recellularization and xenotransplantation after 3 weeks.[27] Although SDS is highly proficient at cellular ablation, acellular scaffolds prepared with SDS have led to adverse cytocompatibility, which has been directly linked to altered matrix composition.[28–32] Therefore, we aimed to develop a new decellularization method using less abrasive detergents, Triton X-100 and sodium deoxycholate. Further, acellular scaffolds can be processed into a solubilized and injectable ovarian-specific ECM (OECM) to facilitate intraovarian follicle transplant.

Here, we report a strategy to enhance intraovarian follicle microinjection using liquid OECM. Injectable OECM was used to facilitate the delivery of allogeneic donor follicles and establish an in situ ovary (ISO) in a chemotherapy treated (CTx) female mouse model to examine the efficacy of donor follicle survival and reproductive outcomes. Transplanted CTx female mice, bred with fertile males, produced donor follicle (green fluorescent protein—GFP+)-derived progeny. Our results confirmed that OECM-facilitated follicle microinjection led to successful engraftment and survival of transplanted follicles. Therefore, this approach offers a minimally invasive method to support and enhance the transplantation of immature follicles to restore reproductive function in female cancer patients.

Results

Biomaterial selection and tissue processing

The damaging effects of chemotherapy on ovarian tissues significantly reduces follicle population, which has a direct impact on fertility and endocrine function.[3–5] In addition, chemical treatments have been implicated in microvasculature and stromal cell irregularities culminating in a compromised environment for cell survival.[3] These unfavorable conditions cause a depletion of ovarian follicles and may reduce follicle viability post-transplantation.[33,34] To re-establish the ovarian tissue microenvironment and repopulate the depleted endogenous follicle pool, we have bioengineered an ISO using an OECM hydrogel to facilitate intraovarian follicle transplant and provide a temporary niche to aid follicle engraftment and survival (Figure 1(a)).

To prepare acellular ovarian scaffolds, porcine ovaries were decellularized using a series of enzymes and detergents to remove immunogenic material (Figure 1(b)–(d)). Tissues transitioned from an initial opaque to translucent appearance at the conclusion of the decellularization steps

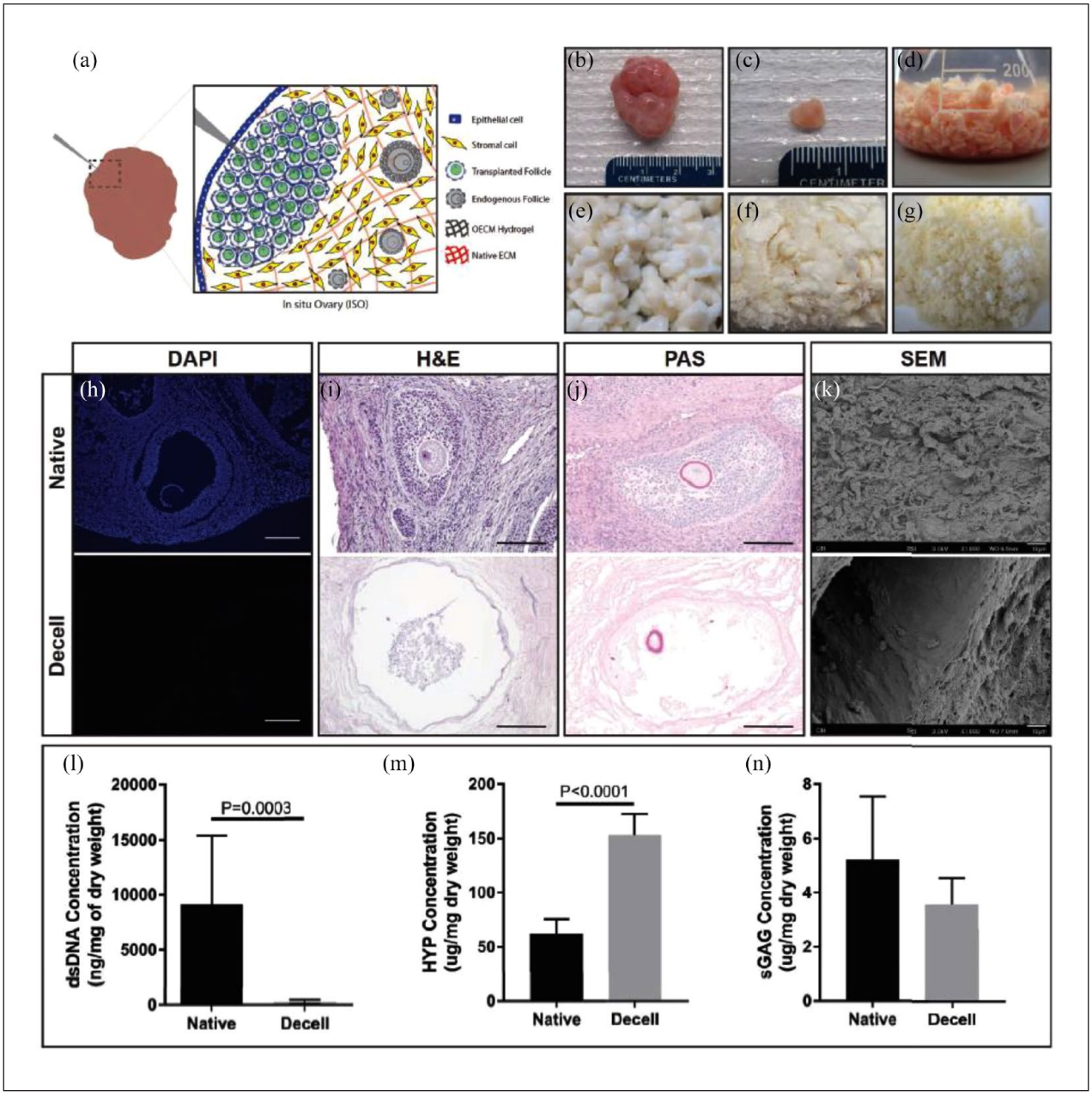

Figure 1. Graphical abstract, decellularization process and tissue characterization. (a) The graphical representation shows our hypothesis for restoring fertility in chemotherapy-treated (CTx) patients. Intraovarian microinjection of an ovarian-specific ECM (OECM) hydrogel can support the delivery and long-term survival of exogenous primordial follicles (green) within an in situ ovary (ISO). The damaged ovarian tissue primarily consists of stromal cells (yellow) and a depleted population of endogenous follicles (gray). (b) Young (<1 year old) porcine ovaries were sourced for decellularization. (c) Ovaries were diced into small cubes (~0.125 cm^3). (d) Cubed ovaries were added to a flask and decellularized using enzymes and detergents. (e) Decellularized ovarian tissues appeared white. (f) Ovaries were frozen then lyophilized to remove their water content. (g) Powdered OECM was prepared using a mill. (h–j) Native (top row) and decellularized (bottom row) images of DAPI (200 µm scale), H&E cellular content (100 µm scale), and periodic acid-Schiff (PAS) (100 µm scale) staining determined that decellularized tissues removed cellular content while preserving ovarian tissue morphology. (k) Scanning electron micrographs (SEM) show a dense cellular ultrastructure in native ovaries in comparison to porous decellularized scaffold (10 µm scale). (l) PicoGreen assay indicated that decellularized ovarian tissues significantly reduced the dsDNA concentration (n = 10). Data represent mean ± s.e.m. of ng/mg dry weight. *p* values by unpaired, two-tailed *t*-test. (m) Hydroxyproline (HYP) concentration was significantly enriched in decellularized tissues ($n = 5$) and (n) sulfated-Glycosaminoglycans (sGAG) levels did not differ significantly between native and decellularized samples ($n = 5$). Data represent mean ± s.e.m. of µg/mg dry weight. *p* values by unpaired, two-tailed *t*-test.

(Figure 1(e)). Ovarian ECM scaffolds were milled into a fine powder prior to biochemical testing and downstream processing (Figure 1(f) and (g)). To demonstrate the effective removal of immunogenic components and preservation of ECM components, we performed a set of histological stains and biochemical assays. Fluorescence staining with 4′,6-diamidino-2-phenylindole (DAPI) showed few, if any nuclei present within the decellularized tissues in comparison to native ovarian tissue controls (Figure 1(h)). Hematoxylin and eosin (H&E) (Figure 1(i)) and Periodic acid-Schiff (PAS) (Figure 1(j)) staining showed a clear retention of ovarian microarchitecture, such as structural aspects of follicles, zona pellucida and corpora lutea, while sparse cellular content was visible. This highlights the effective removal of cellular content, while limiting the disruption of tissue-specific morphology. Scanning electron micrographs (SEM) further detailed the dense cellular content within native ovarian tissues, whereas decellularized tissues appeared to show vacated follicular compartments surrounded by a porous scaffold (Figure 1(k)). A PicoGreen assay demonstrated a greater than 98% reduction of dsDNA between native (9126 ± 1988 ng/mg) and decellularized (262.4 ± 59.96 ng/mg) samples (Figure 1(l)). Gel electrophoresis showed a lack of DNA (Supplemental Figure 1) within the decellularized tissues in comparison to native controls, indicating a reduced potential for disease transmission and adverse immune reaction to cellular contents. Collagen and sulfated glycosaminoglycans (sGAG) were also examined to determine their retention post-decellularization. A hydroxyproline (HYP) assay was used to estimate the total collagen content within the scaffold. Native tissues (61.95 ± 6.064 μg/mg) contained significantly less HYP as a percentage of dry weight than decellularized tissues (153.3 ± 8.564 μg/mg) due to the loss of cellular mass. Under this assumption, the total collagen content within the decellularized scaffold as a fraction of the dry weight of all components was enriched after decellularization (Figure 1(m)). sGAG content was also preserved with no significant difference observed between native (5.24 ± 1.03 μg/mg) and decellularized (3.59 ± 0.436 μg/mg) samples (Figure 1(n)).

Ovarian tissue specificity post-decellularization

The ECM is composed of a tissue-specific milieu of secreted proteins and proteoglycans that support tissue function.[32,35,36] In the ovary, the ECM undergoes dynamic remodeling throughout the reproductive life span and is essential for regulating folliculogenesis and ovulation.[37,38] Specifically, OECM provides mechanical support, maintains normal cell morphology, promotes cell proliferation and steroidogenesis.[38] Additionally, the OECM can sequester hormones and growth factors within the follicle niche to facilitate paracrine and endocrine signaling.[38,39] Therefore, the retention of OECM proteins would be ideal for supporting follicles within the ISO. To determine the effects of decellularization on ECM retention, we characterized a subset of the most highly expressed OECM proteins: Collagen I, Collagen IV, laminin and fibronectin.[37,38,40,41] Immunohistochemistry revealed that Collagen I was distributed uniformly in the native samples, with a slight enrichment surrounding the thecal compartments of the follicles in decellularized samples (Figure 2(a) and Supplemental Figure 2). Collagen IV was also labeled, showing definitive staining within the basement membrane of the epithelial layer and the basal lamina of individual follicles in both the native and decellularized groups (Figure 2(b)). Similar to Collagen IV, laminin was predominantly found within the basal lamina adjacent to the theca interna surrounding follicles (Figure 2(c)). Finally, fibronectin appeared to be conserved throughout the ovarian tissues with little to no differences in distribution between the native and decellularized groups (Figure 2(d)).

Ovarian hormones and growth factors sequestered in the OECM orchestrate both local and systemic endocrine function. The hypothalamic-pituitary-gonadal (HPG) axis stimulates the production of ovarian hormones, which act to modulate hormone production in a cyclic manner.[1] The hypothalamus produces gonadotropin releasing hormone (GnRH), which stimulates the secretion of follicle stimulating hormone (FSH) and luteinizing hormone (LH).[1] FSH and LH trigger the production of estradiol, follicle development and ovulation. Estradiol from the ovulatory follicle and progesterone from the resulting corpus luteum provide feedback to either inhibit or stimulate hormone secretion from the hypothalamus and pituitary.[1] Spatiotemporal production of these reproductive hormones primarily facilitates follicle development, ovulation and pregnancy.[1]

For this study, we were particularly interested in hormones produced by the ovary due to their roles in follicle selection. Specifically, anti-Müllerian hormone (AMH), estradiol and progesterone. AMH is produced by granulosa cells of pre-antral and antral follicles.[42] As AMH levels increase, it can inhibit the recruitment of primordial follicles and decrease the responsiveness of large pre-antral/antral follicles to FSH. AMH is one of the few hormones that are produced during the early stages of folliculogenesis, which are widely recognized as gonadotropin-independent.[43] Estradiol is also produced by follicular cells and is most commonly known for its role in the LH surge which triggers ovulation; however, at low concentrations, estradiol can function as a negative regulator of FSH, which inhibits follicle growth.[43,44] The corpus luteum, which arises from the cells of ovulatory follicles and is present during the late luteal phase, produces high levels of progesterone, which is necessary for maintaining

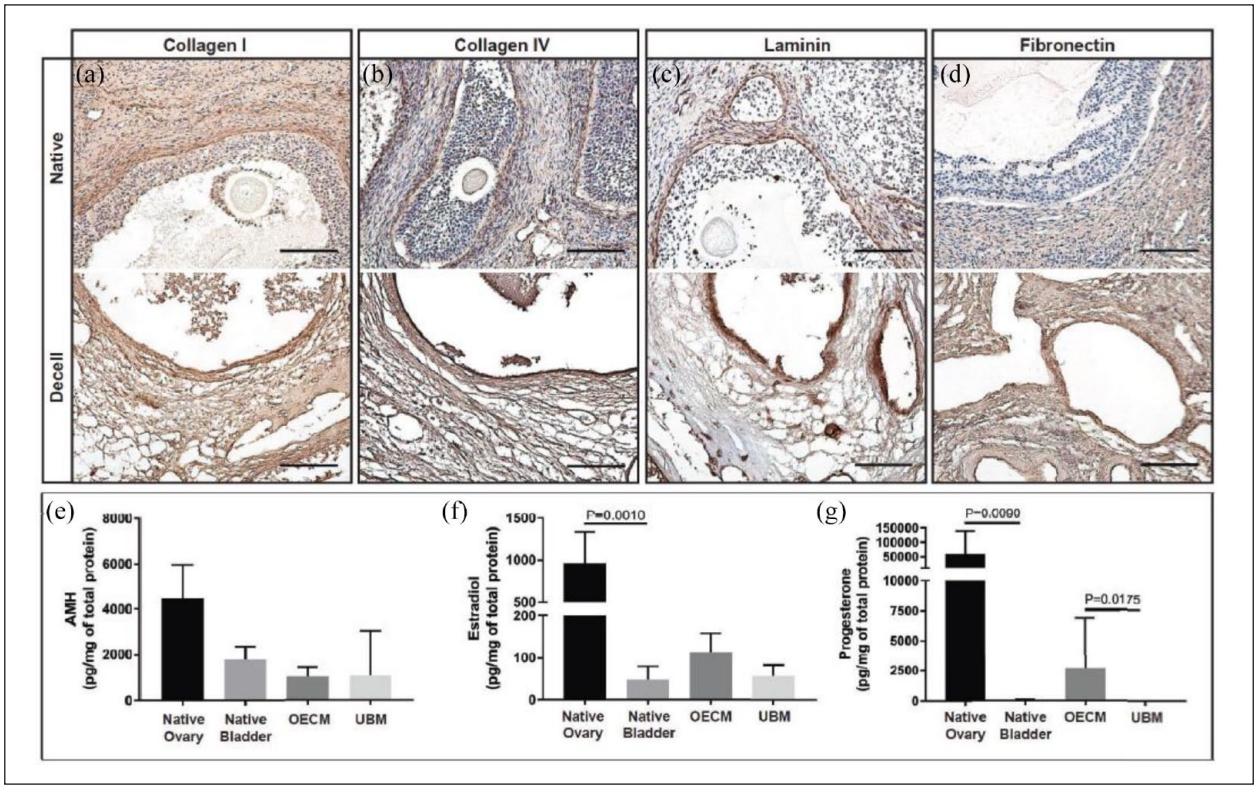

Figure 2. Preservation of ovarian-specific ECM proteins and reproductive hormones. Immunohistochemistry (IHC) images of native (top row) and decellularized (bottom row) ovarian tissues shows the distribution of extracellular matrix proteins: (a) Collagen I was uniformly expressed throughout each of the tissues. (b) Collagen IV appeared to concentrate in the basal lamina of the follicles and the basement membrane surround the epithelial layer of the ovary. (c) Laminin was present within the thecal compartment and (d) Fibronectin was evenly expressed in lower concentrations; however, antibody staining was enriched in decellularized tissues. Scale, 100 μm. Ovarian hormones secreted by follicular cells were quantified from total protein using enzyme-linked immunosorbent assays (ELISAs). (e) Anti-Müllerian hormone (AMH) was measured at high concentrations within native ovarian tissues but was reduced by >50% within decellularized OECM. (f) Estradiol concentrations were significantly higher in native ovary in comparison to native bladder and OECM was two-fold greater than UBM. (g) Progesterone levels were significantly greater in both native ovary and OECM in comparison to native bladder and UBM, respectively. ELISAs were conducted using 100 ovaries batched into five independent samples ($n = 20$ ovaries). Data represent mean ± s.e.m. of pg/mg of total protein. p values by one-way ANOVA using Kruskal-Wallis with Dunn's multiple comparisons test. Native (ovary and bladder) and decellularized groups (OECM and UBM) were compared separately.

pregnancy. Like estradiol, progesterone can also inhibit FSH production further delaying follicle growth.[43]

We hypothesized that these ovarian hormones may be important for the survival of transplanted immature follicles within the ISO. Therefore, to elucidate the effects of decellularization on the disruption of these components, we processed 100 ovaries separated into five groups ($n = 20$ per group) and analyzed as independent samples. As controls, we used both native and decellularized urinary bladder matrix (UBM) collected from female pigs, and prepared as previously described, to determine if there were significant differences in the hormone concentrations based upon tissue source.[45] UBM was selected as a control tissue because bladder shares a common embryonic lineage with the ovary and is known to expresses sex hormone receptors, such as estrogen and progesterone. After tissue homogenization, protein was extracted from each group and tested using biochemical assays for AMH, estradiol and progesterone. ELISA quantification determined that decellularized OECM samples contained low concentrations of each of the ovarian-specific analytes: AMH (1031 ± 192.9 pg/mg), estradiol (113.8 ± 19.63 pg/mg) and progesterone (2697 ± 1890 pg/mg) (Figure 2(e)–(g)). Native ovaries contained significantly higher levels of estradiol and progesterone when compared to native bladder. Furthermore, decellularized OECM had significantly higher progesterone values than UBM. Additional analytes associated with follicle development, insulin-growth factor (IGF-1) and vascular endothelial growth factor (VEGF), were

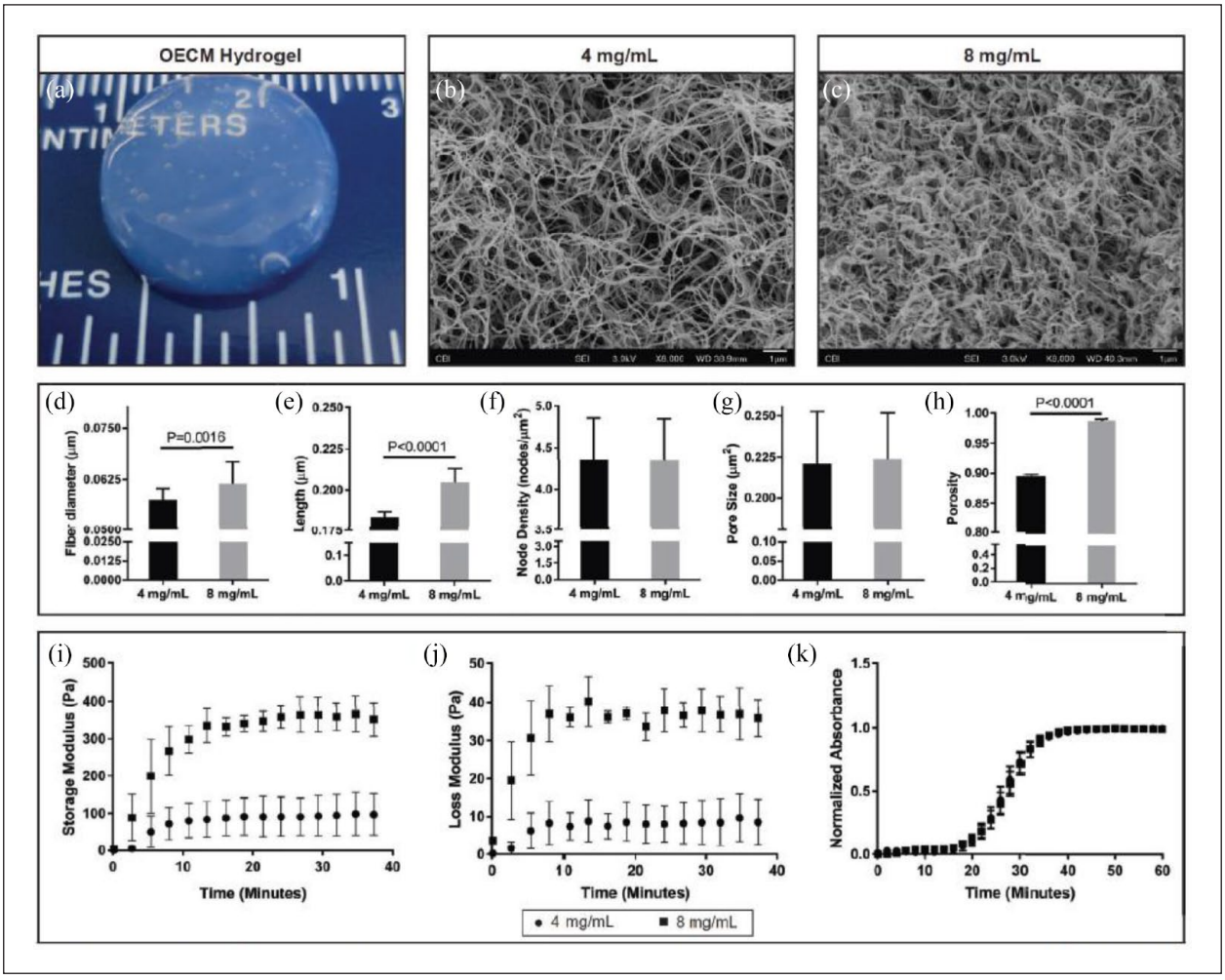

Figure 3. OECM hydrogel preparation, characterization of ultrastructure and viscoelastic properties. (a) Solubilized ovarian ECM (OECM) formed transparent hydrogels upon neutralization and exposure to physiologic conditions. (b and c) Scanning electron micrographs (SEM) show a fibrous and porous architecture at both 4 and 8 mg/mL OECM concentrations. (d–h) Hydrogel fiber network characteristics were quantified using a Matlab algorithm with significant increases in fiber diameter, fiber length and porosity directly correlating with an increase in OECM concentration. Data represent mean ± s.e.m. for all parameters. *p* values by unpaired, two-tailed *t*-test. Viscoelastic material properties were quantified using a rheological time sweep. (i) Storage (G') and (j) Loss (G") moduli increased dramatically with the higher 8 mg/mL OECM concentration. (k) Turbidimetric gelation kinetics showed that gelation was conserved with a change in OECM concentration.

also tested but were undetectable within the decellularized samples (data not shown).

ECM concentration influences ovarian hydrogel properties

Once the decellularized tissues were processed and characterized, we solubilized the OECM then neutralized the digested material to prepare the hydrogels. Visibly transparent hydrogels were formed after exposure to physiological conditions for approximately 20 min (Figure 3(a)). We used SEM to evaluate the hydrogel ultrastructural properties at 4 and 8 mg/mL ECM concentrations (Figure 3(b) and (c)). Fiber network characteristics were quantified using SEM imaging and digital image analysis algorithm.[46] with concentration dependent effects observed with a significant increase in fiber diameter, fiber length and bulk porosity in the 8 mg/mL OECM hydrogel group (Figure 3(d)–(h)). These results indicate that individual fiber and large-scale network properties such as the bulk porosity are dependent on ECM concentration.

To determine the viscoelastic properties of the OECM hydrogel, we performed a rheological time sweep on varying ECM concentrations. An increase in ECM concentration from 4 to 8 mg/mL correlated with an elevated storage (G') and loss (G") moduli (Figure 3(i) and (j)). However, there were no observable differences in turbidimetric gelation kinetics with a change in ECM concentration (Figure 3(k)). Gelation time varied based upon the test conditions. Direct conduction with the Peltier plate achieved complete

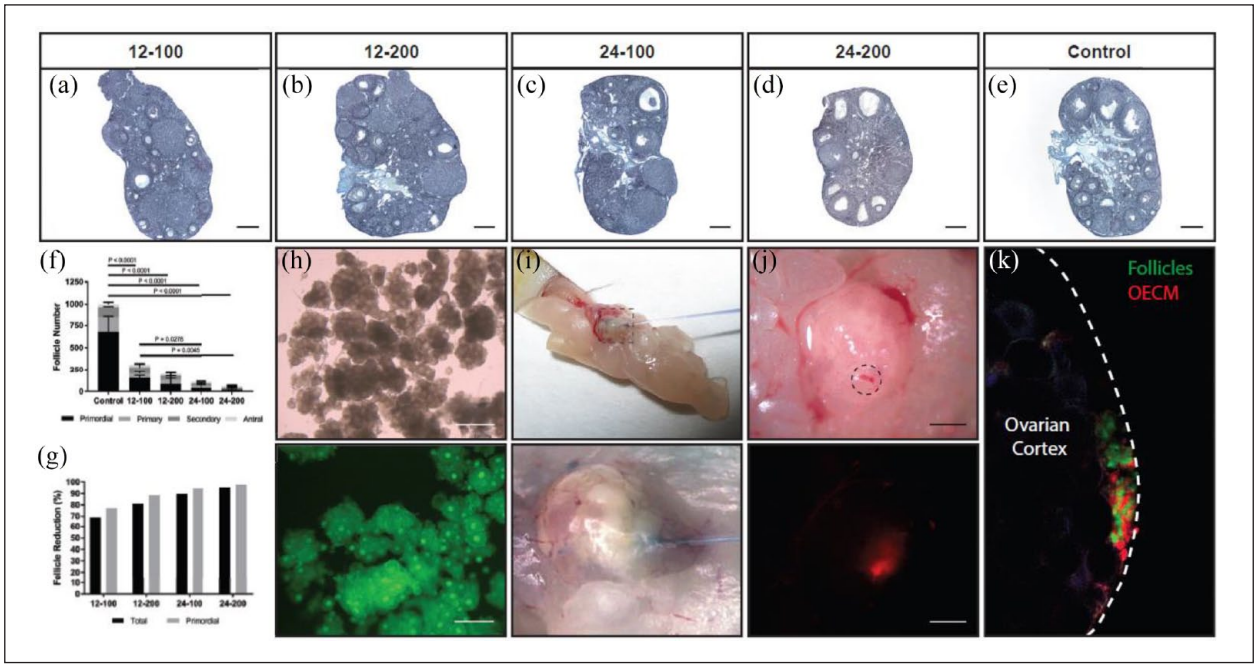

Figure 4. Effects of chemotherapy dose and confirmation of an established in situ ovary (ISO). Four doses of busulfan-cyclophosphamide (a) 12–100 mg/kg (b) 12-200 mg/kg (c) 24–100 mg/kg (d), 24–200 mg/kg (e), non-injected (control) were administered via single IP injection. Ovaries were excised at 3 weeks post-treatment and stained using Weigert's Hematoxylin Picric Acid Methyl Blue. Scale, 250 µm. (f) Follicles were manually counted, quantified, and classified by developmental stage showing a steady decline of the total follicle number with increasing dose. Additionally, busulfan appeared to have an enhanced effect on follicle depletion in comparison to cyclophosphamide. (g) Significant reduction of primordial follicles across all doses indicated a severe depletion of the ovarian reserve, decreasing potential fertility. (h) Intact GFP follicles were enzymatically isolated using Liberase TM and imaged under bright field (top) and fluorescence (bottom). Scale, 500 µm. (i) Brightfield images show the gross morphology of the ovary during microinjection (top) and magnified to show the injection site for follicle transplant (bottom). (j) Pressurized microinjection was tested as a potential technique to deliver the OECM hydrogel (TRITC-labeled) and visualized under bright field (top) and fluorescence (bottom). Scale, 500 µm. (k) Multiphoton images confirmed that intraovarian follicle microinjection of the isolated GFP follicles (green) and OECM (red) co-localized within the ovarian cortex to form an in situ ovary. The dotted line (white) indicates the outer surface of the ovarian epithelium.

gelation approximately 15 min prior to the samples heated via convection during gelation kinetics testing. However, once gelation initiated, hydrogels from both test formats consistently solidified within 20 min.

Alkylating agents significantly reduce endogenous follicle population

After developing and characterizing the OECM hydrogel as a carrier for follicle injection, we created a clinically relevant CTx mouse model. We depleted endogenous follicles using alkylating agents, busulfan and cyclophosphamide, due to their known cytotoxic effects on ovarian tissues and cells.[3,5,47,48] Briefly, a single intraperitoneal (IP) injection was given to 6-week old nude female mice. Dosing was titrated to determine an appropriate treatment that would significantly reduce the endogenous follicle pool to lower or eliminate the chances of fertility. The following doses were tested, abbreviated as busulfan-cyclophosphamide (mg/kg): (1) 12–100 (2) 12–200 (3) 24–100 (4) 24–200.

At 3 weeks post-IP injection, histological staining with Weigert's Hematoxylin-Picric Methyl Blue clearly illustrated the damaging effects of each chemotherapy regimen on the follicle population within the ovaries. Dose dependent effects were observed with elevated levels of busulfan and cyclophosphamide reducing the follicle numbers (Figure 4(a)–(f)). Follicles were counted based upon developmental stage (Supplemental Figure 3). Primordial and primary follicles were significantly reduced after exposure to all treatments in comparison to non-treated control mice (Figure 4(g) and Supplemental Figure 4). The outcomes of chemotherapy titration suggested that a range of doses could impair fertility outcomes or lead to ovarian insufficiency. Therefore, we determined that it was important to evaluate the efficacy of hydrogel-assisted follicle microinjection using female mice treated across each dosage of chemotherapy. We selected the 12–100, 12–200 and 24–100 doses of busulfan-cyclophosphamide to prepare our CTx mice for follicle transplantation because these doses caused significant follicle loss and the animals retained good overall health. Although the 24–200

treatment resulted in the greatest follicle reduction, we excluded this group from follicle transplantation due to the poor health of the mice post-chemotherapy.

Enzymatic follicle isolation and microinjection provides an efficient transplant procedure

Follicle incubation time from isolation to transplant is a concern for cell therapy applications as it can directly impact viability.[49] Therefore, we adapted an existing enzymatic isolation protocol to reduce the time needed to obtain a large pool of immature follicles for transplant.[50] To enable identification of transplanted versus endogenous follicles, we isolated follicles from transgenic mice expressing ubiquitous GFP under the chicken β-actin (CAG) promoter. We tested enzyme concentrations of 10% and 20% for both Liberase TM and DH (13 Wünsch units/mL) to determine their effects on follicle disaggregation and quality. Briefly, Liberase TM or DH was added to the minced ovaries then agitated at 37°C for two 5-min cycles with a minute of pipetting after each cycle. After assessing each sample, we determined that the best formulation was the 10% Liberase TM, which released a large population of morphologically normal GFP follicles during the 12-minute isolation procedure (Figure 4(h)). The other treatments were not evaluated further due to insufficient digestion or over-digestion. To estimate the number of follicles isolated with this procedure, follicles were manually counted using a hemocytometer (Supplemental Figure 5). There were approximately 1.5×10^3 total follicles isolated per ovary with 74.4% of this population identified at the primordial stage.

Once it was feasible to efficiently obtain follicles, we tested the efficacy of microinjection to transplant follicles into the ovarian cortex of CTx mice. Immature follicles naturally reside within the ovarian cortex, as this region of the ovary has mechanically distinct properties that support maintenance of immature follicles.[34,51] Therefore, we wanted to precisely dispense follicles into or near the cortex. Previously, intragonadal cell delivery has been successful using microinjection.[15–17] Therfore, we implemented this technique to facilitate intraovarian follicle transplant to establish an ISO. First, we tested the delivery of the OECM hydrogel alone via microinjection. A small volume of hydrogel was injected into the ovarian cortex, and the recipient animal was sacrificed to visualize the injection site (Figure 4(i)). Bright field images clearly illustrated Trypan blue dye at the site of injection at the tissue surface (Figure 4(j)). Furthermore, the use of a TRITC-labeled OECM hydrogel allowed us to identify the hydrogel at the ovarian surface post-injection (Figure 4(j)). These results confirmed this method as a suitable delivery mechanism for the viscous OECM within a specific anatomical location of the ovary. We performed the same experiment with the addition of isolated GFP follicles to determine if the gel and follicles could be delivered simultaneously, resulting in the formation of an ISO. Ovaries excised from the TRITC-OECM hydrogel and GFP follicle microinjection clearly indicated a co-localization of the OECM and follicles within the ovarian cortex (Figure 4(k)).

Microinjected follicles give rise to multiple generations of GFP-expressing pups

We used CTx mice to investigate the therapeutic potential of an ISO to support follicle survival after intraovarian microinjection. Approximately 1.0×10^3 GFP+ follicles resuspended in OECM hydrogel were microinjected into the ovarian cortex of CTx nude female mice exposed to varying amounts of alkylating agents: 12–100 ($n=2$), 12–200 ($n=2$) and 24–100 ($n=2$). Non-injected CTx nude female mice were used as controls: 12–100 ($n=3$), 12–200 ($n=2$) and 24–100 ($n=2$). To reduce tissue damage due to needle puncture, only a single follicle injection was performed on each ovary. Freshly isolated GFP follicles from 6 to 14 days female (DBA-GFP/nu−) mice were used to ensure a predominantly immature follicle population at the time of injection.

To determine the effects of follicle microinjection on fertility, follicle recipient and non-injected control CTx nude female mice were mated with nude male mice for three breeding cycles (~100 days). The breeding strategy was designed to distinguish between pups derived from transplanted or endogenous follicles (Supplemental Figure 6a). Pups from endogenous follicles would be nude, lacking fur, whereas pups from transplanted GFP follicles would have fur with a 50% chance of GFP expression (GFP/nu−). After three breeding cycles, CTx follicle transplant recipients produced a total of three GFP+/nu− pups within three separate litters (Supplemental Figure 6b). The first breeding cycle yielded one GFP pup (GFP/nu−001) out of three healthy offspring followed by a single GFP pup (GFP/nu−002) with no littermates during the second cycle (Figure 5(a) and (b)). As a note, when litters were small, the pups were fostered into nude litters (as shown by the additional nude pups in Figure 5(b)). Each of the first two GFP pups were born from the same CTx mouse treated with a dose of 24–100 mg/kg. This observation demonstrates that intraovarian follicle transplant has the potential to lead to multiple births from a single injection. During the third and final breeding cycle, one GFP pup (GFP/nu−003) was born out of five healthy offspring from a CTx mouse in the 12 to 100 mg/kg group (Figure 5(c)). These results suggest that transplanted follicles are viable for at least 90 days post-injection. Overall, eight litters and a total of 35 pups were born from CTx mice that received a follicle transplant ($n=6$). In comparison, seven litters with a total of 36 pups were born from non-injected CTx control mice ($n=7$). Although OECM-facilitated follicle microinjection did not increase the total offspring, this

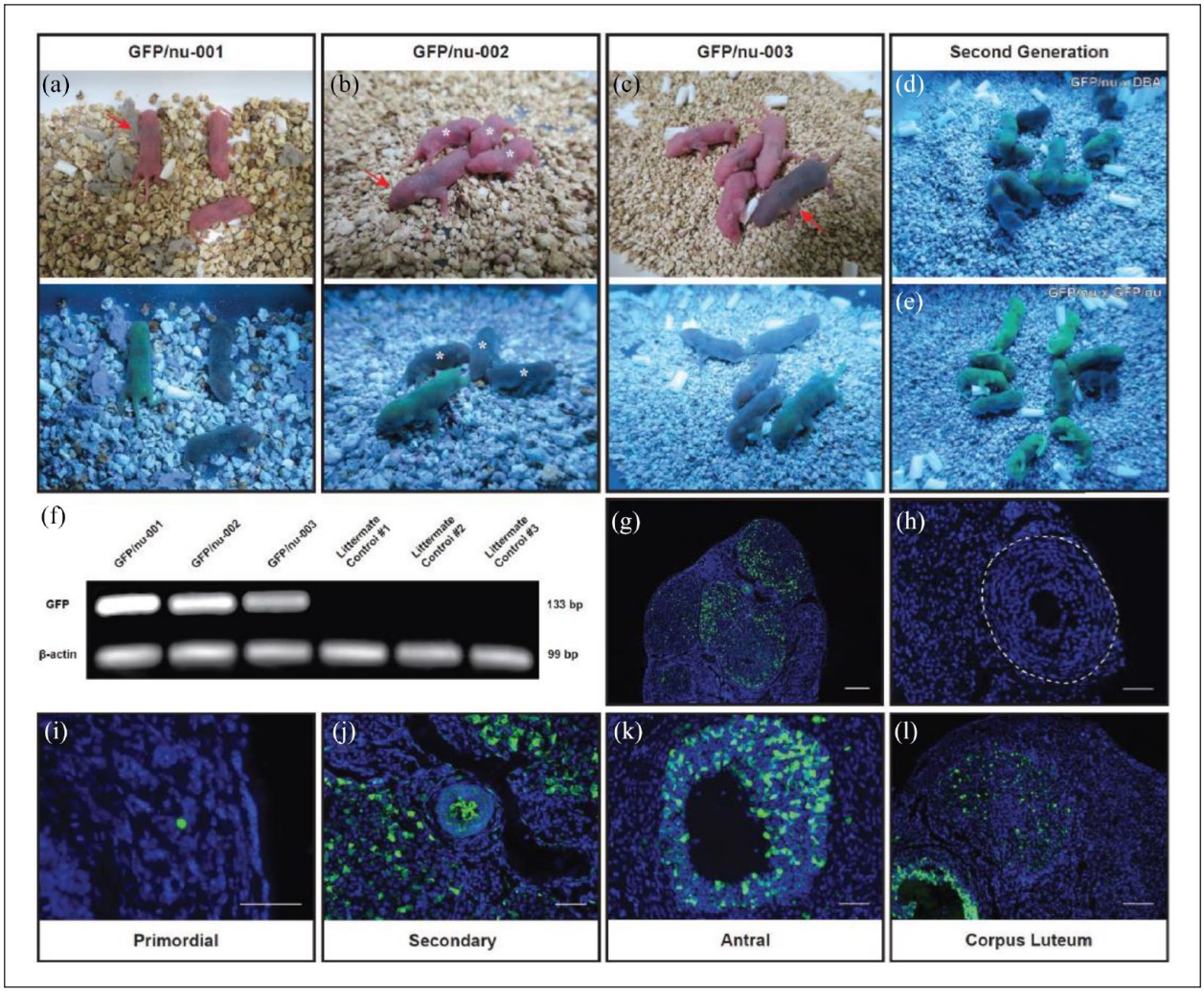

Figure 5. Intraovarian transplant gives rise to GFP offspring and supports follicle longevity. The efficacy of intraovarian follicle transplant for fertility preservation was tested by injecting a pool of isolated GFP follicles within an OECM hydrogel into a CTx nude female mice. The follicle recipient mice were then mated to male mice of the same genetic background (nu/nu) to distinguish between progeny derived from exogenous (GFP+) or endogenous (GFP−) follicles. (a and b) Two GFP pups (GFP/nu−001 and GFP/nu−002) were born in consecutive litters from the same mother (24 to 100 mg/kg dose) as a direct result of the follicle transplantation. (c) Another GFP pup (GFP/nu−003) was derived from a CTx female mouse (12 to 100 mg/kg dose) during the third mating cycle (>100 days post-transplant). This demonstrates that an ISO can support the engraftment and long-term viability of follicles post-injection. Multiple litters of second-generation pups were derived from both (d), outbred (GFP/nu × DBA) and (e) inbred (GFP/nu × GFP/nu) mice, which indicates that intraovarian follicle transplantation did not disrupt reproductive development. (f) Genotyping of the GFP pups and littermate controls was confirmed using standard PCR and gel electrophoresis. GFP bands only appeared within the GFP mouse samples and none within the littermate samples. β-actin was used as an internal control appearing in each of the samples tested. Gels were cropped and processed to highlight the bands of interest. Ovarian tissues were excised from CTx follicle recipient mice after three breeding cycles (106 days on average). Immunofluorescence staining was performed using DAPI (endogenous cells) and GFP (transplanted cells) to evaluate follicle survival. (g) A representative image of a transplanted ovary suggests that GFP+ cells integrated within the tissues and were actively proliferating. Scale, 200 μm. (h) Presence of an endogenous secondary follicle (GFP−), indicated by dotted line (white). Scale, 50 μm. Various stages of follicle development were also present among the transplanted tissues, including: (i) Primordial (Scale, 50 μm) (j) Secondary (Scale, 50 μm) (k) Antral (Scale, 50 μm), and (l) Corpus Luteum (Scale, 100 μm).

method supports the transplantation, engraftment, and survival of isolated follicles within a compromised ovarian microenvironment. To assess the need for a biomaterial-assisted delivery, we performed the same follicle microinjection with saline into CTx mice. In the absence of OECM, follicle-transplanted CTx mice ($n=6$) produced 13 total pups (12 live and 1 dead); however, these mice failed to produce any GFP^+ pups (Supplemental Figure 7). These findings would suggest that a biomaterial vehicle is critical in both the engraftment and survival of transplanted follicles.

A follow-up mating study was performed to test the reproductive health of the GFP pups generated from follicle transplantation. The GFP offspring resulting from follicle transplant (DBA-GFP+/nu−) were bred with DBA wild-type (GFP−/nu+) (Supplemental Figure 6c) and inbred with each mating pair (Supplemental Figure 6d) producing multiple litters of hemizygous (GFP+/−) and homozygous (GFP+/+) genetic backgrounds (Figure 5(d) and Supplemental Figure 6e). In each of the litters, GFP expression was clearly observed and confirmed with genotyping (Figure 5(f)).

Intraovarian microinjection supports follicle longevity post-transplant

Finally, we wanted to determine the effects of this therapy on follicle longevity post-transplant. To answer this question, we performed immunofluorescent labeling of ovaries excised from CTx nude female mice after three breeding cycles (~100 days). Comprehensive imaging demonstrated significant GFP expression throughout the transplanted tissues and suggests that multiple follicles remained viable post-transplantation (Figure 5(g)). Transplanted ovaries also retained growing endogenous follicles (Figure 5(h)). Non-injected control tissues lacked GFP expression and endogenous follicles appeared to be reduced in comparison to ovaries from transplanted mice (Supplemental Figure 8). However, we could not confirm any definitive differences between residual endogenous follicles based solely upon the immunofluorescence images. Finally, we were able to identify follicles at various stages of development including primordial (Figure 5(i)), secondary (Figure 5(j)), antral (Figure 5(k)), and corpus luteum (Figure 5(l)), which indicates that the ISO is compatible with engraftment and long-term development of transplanted follicles.

Discussion

Women who cryopreserve oocytes or embryos prior to gonadotoxic treatments can use assisted-reproductive technologies (ART), such as IVF and embryo transfer to start a family.[52,53] To preserve eggs or embryos, the patient must first undergo hormone stimulation to collect mature oocytes. Controlled ovarian stimulation requires two or more weeks and is not a viable option for patients who have not reached reproductive maturity or who cannot afford to postpone treatment.[54–56] For these individuals, cryopreservation of ovarian cortex prior to treatment is the only potential option to naturally restore endocrine function and fertility.

The current gold standard for fertility preservation in patients in remission is the autologous surgical transplantation of cryopreserved, thawed ovarian cortical strips.[6,8,11–14,57–62] To date, there have been numerous successful procedures performed in humans, resulting in 189 live-births; however, the efficiency of this method could be improved, with live-birth rates ranging from 28% to 45% after transplantation of frozen and fresh ovarian tissues, respectively.[63] Although ovarian tissue transplantation has shown promise, it is an invasive procedure and carries a potential risk of reintroducing malignant cells back into the body.[64] To address these concerns, several pre-clinical experimental approaches have been proposed, including in vitro follicle maturation (IVM), the development of an artificial ovary and stem cell transplantation (Table 1).

IVM consists of the isolation and culture of immature follicles to obtain meiotically-competent oocytes for IVF. IVM approaches have predominantly shifted from two-dimensional culture toward three-dimensional hydrogel-based follicle encapsulation, which has improved follicle morphology and intercellular signaling.[72] The most commonly used hydrogel for IVM is alginate.[9,73–79] There are several other options that have been examined including, fibrin,[80] fibrin-alginate,[71,81] polyethylene glycol (PEG).[82,83] Each of these materials provide a unique set of physical and biochemical properties, which allows them to support the growth and maturation of follicles in vitro. Successful application of IVMhas been shown in mice leading to live-births [78]; however, the pre-clinical translation of this approach for human follicles has been limited.[84] Recently, follicle maturation has been attempted in vivo through the heterotopic subcutaneous transplant of a retrievable hydrogel seeded with immature follicles.[66] Antral follicles developed in the hydrogel and germinal vesicle stage oocytes could be extracted, matured to MII stage, and fertilized, leading to the development of two- and four-cell embryos. However, in this study, embryos were not transferred, and pregnancies were not established.

As IVM has proven to be a major challenge for human follicles, several groups have pursued the development of an artificial ovary. This concept involves the isolation and sequestering of immature follicles in a bio-supportive scaffold that can be transplanted to recover ovarian function. Similar to IVM, various biomaterials are being examined as options to support the delivery, survival and function of ovarian follicles in vivo. Recently, a fibrin gel supplemented with vascular endothelial growth factor (VEGF) was used to facilitate the transplantation of primordial follicles into the bursa of ovariectomized mice and gave rise to a healthy litter of pups.[68] In another study, 3D printed gelatin scaffolds were used to examine the effects of pore geometry on follicle survival and achieved healthy pups through natural mating post-implantation in sterilized mice.[33] Since each of these studies used ovariectomized mice as transplant recipients, they were unable to evaluate the suitability of the endogenous ovary as a transplant site or the impact that chemotherapy would have on transplant follicle engraftment, survival and development.

Table 1. Summary of notable pre-clinical experimental therapies and their future outlook for fertility preservation.

Approach	Source material	Processed form	Study type	Model of infertility	Summary	Reference
Ovarian engraftment	Healthy Ovarian Tissue	N/A	In vivo	Yes (Chemotherapy)	Batchvarov et al. use a chemotherapy regimen of busulfan and cyclophosphamide to induce infertility. Grafted ovarian tissue was able to rescue host fertility although non-grafted hosts also gave rise to litters 200+ days post treatment.	Batchvarov et al.[65]
Biomaterial-facilitated	Sodium Alginate	Alginate gel	In vivo	No	Rios et al. examine the potential of immunoisolating and encapsulating ovarian follicles within alginate hydrogels for subcutaneous transplant. Hydrogels were retrieved and mature oocytes were collected then successfully fertilized with 7% of the embryos reaching 4 cell stage.	Rios et al.[66]
	Human Ovary	OECM Scaffold	In vitro/ In vivo	No	Hassanpour et al. develop a decellularization protocol incorporating SLES to prepare an ovarian tissue specific scaffold.	Hassanpour et al.[67]
	Gelatin	3D Printed Scaffold	In vivo	Yes (Ovariectomy)	Laronda et al. establish a bioprosthetic 3D printed ovary to restore ovarian function in sterilized mice. GFP pups born from exogenous follicle transplant.	Laronda et al.[33]
	Synthetic PEG	PEG hydrogel	In vivo	Yes (Ovariectomy)	Kim et al. implement a PEG-VS hydrogel to support the transplantation of immature follicles and restore endocrine function for up to 60 days.	Kim et al.[50]
	Fibrinogen/ Thrombin	Fibrin gel	In vivo	No	Paulini et al. test an artificial ovary using a fibrin gel showing the efficacy of xenografting isolated preantral follicles within the peritoneum. Results showed follicles survival and proliferation up to 7 days post-transplant.	Paulini et al.[7]
	Human/ Bovine Ovary	OECM Scaffold	In vivo	Yes (Ovariectomy)	Laronda et al. detail a procedure for the decellularization of both human and bovine ovaries. Primary ovarian cells seeded onto decellularized grafts were transplanted into ovariectomized mice and showed evidence of initiating puberty.	Laronda et al.[25]
	Fibrinogen/ Thrombin	Fibrin gel + VEGF	In vitro/ In vivo	Yes (Ovariectomy)	Kniazeva et al. test several biomaterial graft systems in an ovariectomized mouse. Successful litters resulted solely from fibrin gel supplemented with VEGF.	Kniazeva et al.[68]
	Fibrinogen/Thrombin	Fibrin gel	In vivo	Yes (Ovariectomy)	Smith et al. characterize the use of a fibrin gel for the transplant of ovarian follicles. Early-stage follicles were enzymatically isolated, encapsulated within fibrin gels and transplanted into an ovariectomized mouse. Tissue explants were performed at 0, 3, 9 and 21 days with follicles populations being significantly reduced by day 9.	Smith et al.[69]
	Fibrinogen/Thrombin	Fibrin gel	In vivo	Yes (Ovariectomy)	Luyckx et al. prepare an artificial ovary from fibrin gel that promotes survival and proliferation of preantral follicles 1 week post-transplant.	Luyckx et al.[70]
	Fibrinogen/Thrombin	Fibrin gel + VEGF	In vivo	Yes (Ovariectomy)	Shikanov et al. introduce a combination system consisting of Fibrin gel supplemented with VEGF to stimulate angiogenesis and promote graft survival. Transplanted mouse ovarian tissues supported by the Fibrin/VEGF material improved follicle survival when compared to no biomaterial control. The transplant material was also able to give rise to a litter of pups.	Shikanov et al.[71]
Intraovarian Transplantation	Female germline stem cells (FGSCs)	PBS	In vivo	Yes (Chemotherapy)	Xiong et al. implement a stem cell therapy to reverse the effects observed with exposure to chemotherapy. FGSC microinjection led to healthy pups post-chemotherapy.	Xiong et al.[15]
	Primordial Follicles	PBS	In vivo	Yes (Chemotherapy)	Park et al. show significant genetic changes within primordial follicle markers after exposure to chemotherapy. Intraovarian primordial follicle transplantation did not restore fertility.	Park et al.[20]

Several therapeutic approaches have been explored to ameliorate the effects of infertility. In general, these can be divided into three main categories: (1) Ovarian engraftment, (2) Biomaterial-facilitated and (3) Intraovarian transplantation methods. Ovarian engraftment can be equated to cortical strip auto transplantation, which is currently considered as the gold-standard in the field. Biomaterial-facilitated methods have recently progressed toward the development of a functional artificial ovary, which uses a scaffold or hydrogel to support follicle transplantation. Intraovarian transplantation has been the primary focus for the delivery of oogonial stem cells (OSCs). Each of the in vivo studies listed have used varied models of infertility, induced either by ovariectomy or chemotherapy, with a limited number showing the ability to produce pups (highlighted in green). However, the clinical translation of these approaches may be hindered by invasive surgical procedures and ex vivo follicle and stem cell manipulation. To overcome these barriers to the clinic, we have proposed a minimally invasive technique to facilitate the delivery and support of ovarian follicles within an in situ ovary (ISO), which promotes a natural solution for restoring fertility.

The objective of this study was to develop a method to transplant ovarian follicles into the endogenous ovary using a supportive OECM hydrogel. This approach requires minimal in vitro manipulation of follicles and short-term exposure to ex vivo conditions prior to intraovarian microinjection. To aid in delivery and engraftment of follicles, we developed a solubilized acellular ovarian scaffold to create a thermo-responsive, injectable material which formed in situ under physiological conditions. In addition, we proposed an adapted method to efficiently isolate follicles to reduce the total time ex vivo prior to transplantation. To mimic the effects of clinical CTx, a single intraperitoneal injection of busulfan and cyclophosphamide was used to significantly reduce the endogenous follicle population in female recipient mice. The OECM hydrogel combined with freshly isolated GFP^+ ovarian follicles were successfully delivered into the ovarian cortex, forming an ISO. Intraovarian follicle transplant aided by the OECM hydrogel gave rise to multiple, consecutive litters containing at least one pup expressing GFP.

This study demonstrates a potential strategy for restoring fertility after chemotherapy, however, we acknowledge that there are several limitations. Although the use of ovarian-specific ECM hydrogels demonstrates utility as a follicle delivery vehicle and supportive matrix post-transplant, the bioactivity of hormones/GFs detected post-decellularization may be altered or degraded during downstream processing (e.g. enzymatic digestion). Further elucidating the role of ovarian specificity in fertility outcomes post-transplant could be probed using a non-tissue specific biomaterial and/or purified ECM subtype, such as Type I Collagen.

A major benefit of isolating follicles from the ovarian stroma is the potential to reduce malignant cells that could be introduced during transplantation.[68,85] Here, we developed an enzymatic method to rapidly obtain a high-density population of follicles. Although we counted and classified the follicles by developmental stage, we did not perform assays to directly assess follicle function prior to transplantation. However, this was confirmed indirectly through the birth of healthy GFP pups. To improve the reproducibility and success of this approach, viability and/or other functional assessments should be performed to consistently evaluate reproductive outcomes after orthotopic follicle injection. Additionally, since our primary aim was to evaluate the method of intraovarian follicle transplant, we did not filter out stromal cells within our follicle suspension after isolation. Therefore, it is possible that stromal cells or other cell types may have contributed to ovarian follicle survival within the CTx ovaries. Further, donor follicles were isolated from whole allogeneic ovaries rather than autologously sourced ovarian tissue. We also used a wide follicle donor age range (6–14 days), which could yield different follicle and stromal cell populations. In future experiments, it would be ideal to use donor mice from the same age to reduce variability. To increase the number of available donor follicles, isolated follicles were combined into a single batch and equally distributed for transplantation.

A future goal of this approach is to provide a therapeutic platform for the transplantation of cryopreserved, autologous follicles to restore fertility in human patients. In this initial study, we examined the effects of this method on donor follicle survival after intraovarian microinjection using immune-compromised CTx mice. Although the CTx mice had a significantly reduced follicle number they were not infertile, as non-injected control mice had multiple litters. In addition, the presence of endogenous follicles could aid exogenous follicle integration and survival within the ovarian niche. Another significant limitation of this study was the size of the mouse ovaries. The current animal model restricted the use of larger volumes of injected gel during a single treatment making it difficult to deliver a greater quantity of follicles. Theoretically, as the number of injected follicles increases fertility outcomes may improve. Further, the ratio of gel to follicles may also be a decisive factor in long-term follicle survival. For example, a higher follicle concentration could inhibit access to nutrients within the ISO, triggering apoptosis or atresia. To improve upon the current outcomes, we propose testing multiple hydrogels with varied composition and mechanical properties to evaluate in situ follicle-hydrogel interactions over time. To this end, a comprehensive follow up study should be conducted in a large animal model using follicles isolated from cryopreserved, autologous ovarian tissues to evaluate the therapeutic and translational potential of this approach.

Here, we demonstrate that OECM hydrogels, paired with intraovarian microinjection, can provide a suitable environment to support the engraftment and survival of transplanted follicles after chemotherapy. Chemotherapeutic agents alter the follicle milieu by disrupting developing follicles, along with their supportive vasculature, and inducing fibrosis. This therapeutic approach employs the unique biochemical and mechanical properties of the OECM to establish an ISO within a damaged and unsupportive ovarian microenvironment. We postulate that this technique could be deployed clinically using a minimally-invasive ultrasound-guided approach, similar to what is currently used to aspirate follicles from the ovary in preparation for IVF. However, instead of aspirating eggs, follicles could be injected directly into the ovarian cortex. The restorative reproductive outcomes observed in this study suggest that this platform could be used as a natural, alternative approach for fertility preservation.

Materials and methods

Ovarian tissue decellularization

Porcine ovaries from adolescent pigs (<1 year old) were obtained from the local abattoir (*Thoma Meat Market, Saxonburg, PA*) and immediately stored on ice and frozen

at −20°C. Ovaries were thawed, cleared of surrounding connective and adipose tissues, diced into cubes (~0.125 cm^3) and transferred to a flask containing cold Milli-Q water (MQ). The diced tissues were shaken manually with MQ until residual blood was visibly removed then replaced with fresh MQ and stored overnight at 4°C. The tissues were rinsed in fresh MQ on an orbital shaker for 30 min at 300 rpm. The flask containing tissue was replaced with a pre-warmed solution of 0.02% trypsin/0.05% EDTA and agitated on a magnetic stir plate for 1 h at 37°C. Ovaries were rinsed three times with MQ for 15 min each at 300 rpm. A 3% solution of Triton X-100 was added to the flask and shaken for 1 h at 300 rpm. A subsequent wash cycle was implemented to remove any residual detergents from the tissues. Each wash cycle consisted of several distilled water rinses with manual shaking (until no bubbles were observed), followed by alternating washes of MQ and 1X PBS to neutralize and release detergent that was bound to the tissues. After the wash cycle was completed, the fluid was replaced with fresh MQ and stored overnight at 4°C. A 4% sodium deoxycholate solution was added to the flask and agitated for 1 h at 300 rpm. A subsequent wash cycle was performed and the tissue was replaced with fresh MQ and stored overnight at 4°C. The ovarian tissues were depyrogenated and disinfected with a 0.1% peracetic acid and 4% ethanol solution for 2 h at 300 rpm. This step was followed by three rinses in MQ, 1X PBS, MQ for 15 min each at 300 rpm then stored in fresh MQ at 4°C overnight. To ensure adequate removal of detergents and other chemical reagents one final series of washes with MQ, 1X PBS, MQ were performed for 15 min each at 300 rpm. The decellularized tissues were then stored at −80°C prior to lyophilization. The rationale for using porcine tissues as an ECM source was their relatively conserved matrisome homology with other mammalian species. In addition, porcine ovaries mimic the structural organization and similar biochemical composition of mouse and human ovaries. Porcine ovaries offer a significantly larger tissue source, which substantially increases ECM yield per ovary.

Characterization of decellularized tissues

Decellularized ovarian tissues were characterized using a number of qualitative and quantitative measures to verify the removal of genetic material and maintenance of ovarian specific proteins. Native and decellularized ovarian tissues were formalin-fixed, paraffin-embedded, sectioned and stained using several histological procedures including DAPI (4′,6-diamidino-2-phenylindole), Hematoxylin and Eosin (H&E), and Periodic Acid-Schiff (PAS). Antibodies specific for ECM proteins Collagen I (Abcam, ab34710) and IV (Abcam, ab6586), Fibronectin (Abcam, ab23751), and Laminin (Abcam, ab11575) were evaluated using DAB (3,3′-Diaminobenzidine) immunohistochemistry (IHC) staining to show conservation after decellularization. IHC tissue sections were counterstained using Hematoxylin QS (Vector Labs, Cat No. H-3404) to highlight nuclei in contrast with resident ECM proteins. DNA removal was quantified using a PicoGreen dsDNA assay kit (Invitrogen, Cat No. P11496). A 2.5% agarose gel was used to detect DNA fragments at a resolution between 25 and 1000 bp. Hydroxyproline (HYP) and sulfated glycosaminoglycans (sGAG) assays were performed to detect collagen and sGAG content. Native and decellularized ovarian tissues were homogenized in a High Salt Buffer (pH 7.5, 50 mM Tris base, 150 mM NaCl, 5 M $CaCl_2$, 1% Triton-X-100, 1% Halt protease inhibitor cocktail, Pierce Biotechnology, Rockford, IL). Protein concentrations of the extracted tissues were determined using the BCA Protein Assay Kit (Pierce Biotechnology, Rockford, IL) and 50 μg total protein was used per sample for all assays. Ovarian specific growth factors including insulin growth factor (IGF-1) (R&D Systems, Minneapolis, MN), 17β-estradiol (R&D Systems, Minneapolis, MN), progesterone (Abcam, Cambridge, MA), anti-Müllerian hormone (AMH) (R&D Systems, Minneapolis, MN), and vascular endothelial growth factor (VEGF) (Abcam, Cambridge, MA), were quantified using enzyme-linked immunosorbent assays (ELISA).

Ovarian ECM digestion and hydrogel formation

Lyophilized ovarian ECM powder was solubilized via enzymatic digestion. A stock ECM digest concentration of 10 mg/mL was prepared by adding 200 mg of ECM powder to a 20 mL solution of pepsin (Sigma P7012) at a concentration of 1 mg/mL (⩾2500 units/mg) dissolved in 0.01 N hydrochloric acid (HCl). Digestion was facilitated with an overhead mixer between 700 and 2000 rpm for less than 48 h. Hydrogels were formed after neutralizing and buffering the solubilized ovarian ECM to physiological conditions. Two hydrogel concentrations (4 and 8 mg/mL) were prepared for testing and experimentation. A pre-gel solution was made on ice using the following components: (i) 10 mg/mL OECM digest stock (volume determined by desired final concentration) (ii) 0.1 N NaOH (1/10th the volume of the digest), (iii) 10X PBS (1/9th the volume of the digest), and (iv) 1X PBS or L-15 medium (brought up to final volume). The solution was pulsed three times on a vortexer to mix then stored at 4°C until further use.

Hydrogel characterization

Ovarian hydrogel ultrastructure was assessed using scanning electron microscopy (SEM). Hydrogels were fixed using 2.5% glutaraldehyde, washed with 1X PBS and post-fixed with osmium tetroxide (OsO_4). Samples were washed

again in 1X PBS to dilute the OsO_4, then they were slowly exsiccated through a series of increasing ethanol concentrations. Complete dehydration was achieved using a critical point dryer. Dried hydrogels were sputter-coated with gold/palladium particles and imaged at 8000× magnification. A proprietary Matlab code was used to analyze SEM images to determine various hydrogel fiber network characteristics. Ovarian hydrogel bulk viscoelastic properties were determined using a dynamic parallel plate (40 mm) rheometer (AR-2000 TA instruments). A time sweep (5% strain, 1 rad/s) was used to demonstrate the effect of ECM concentration on both the storage (G') and loss (G") modulus. Turbidimetric gelation kinetics were performed on the ovarian hydrogels as previously described.[86,87]

Chemotherapy-treated (CTx) mouse model

Busulfan (Sigma) and cyclophosphamide (MP BioMedicals LLC) were combined to significantly reduce the ovarian follicle reserve in 6-week old female mice (NCR nu/nu). Recipient mice were given a single intraperitoneal injection (IP) and allowed to recover up to 3 weeks prior to treatment. To initially identify the most appropriate chemotherapy regimen, four doses of busulfan/cyclophosphamide (mg/kg) were tested: (1) 12–100 (2) 12–200 (3) 24–100 (4) 24–200. Ovaries were excised, fixed in 4% paraformaldehyde (PFA), paraffin embedded, and serial sectioned. Tissue sections were stained using Weigert's Hematoxylin Picric acid Methyl Blue then imaged under an upright brightfield microscope. Every 10 sections were examined for total follicle number, classified by stage, and quantified. The following criteria were used to count the follicles: (1) each follicle contains a visible oocyte, (2) primordial follicles have a single layer of squamous granulosa cells, (3) primary follicles have single layer of cuboidal granulosa cells, (4) secondary follicles contain two to four layers of granulosa cells without the development of an antrum, and (5) antral follicles have greater than four layers of granulosa cells as well as definitive antrum. The total number of follicles were quantified, and the sum was multiplied by 10 to provide an estimate of the entire follicle population of each ovary.

Enzymatic follicle isolation

Ovarian donor follicles were prepared using a physical and enzymatic isolation procedure adapted from Kim et al.[50] First, ovaries were excised from 6 to 14 days old female (DBA GFP/nu) mice and placed into pre-warmed L-15 (Leibovitz's) medium. The ovaries were freed from the bursa using a pair of forceps and an insulin needle. Ovaries were then minced using insulin needles into small fragments to aid in digestion. The ovarian fragments were added to 1.5 mL microcentrifuge tube containing 500 μL of pre-warmed L-15 medium and 50 μL of Liberase TM (13 Wünsch units/mL). The tubes were placed on an orbital shaker and agitated at 200 rpm for 5 min at 37°C. After incubation, the mixture was pipetted gently for 1 min to help free the ovarian follicles from connective tissue. This process was repeated once more until the ovaries had been completely dissociated. After digestion, 10% fetal bovine serum was added to the mixture to halt enzyme activity. The tubes were placed in an upright position for 15 min at 37°C to allow follicles to settle. After 15 min, 200 μL of the mixture was carefully pipetted off the top to remove singular ovarian cells. The samples were centrifuged at 100*g* for 5 min to loosely concentrate the follicles. A syringe needle was used to gently remove the medium from the tube without disturbing the follicle pellet. Finally, the pellet was resuspended in a chilled 4 mg/mL OECM pre-gel and kept on ice in preparation for follicle microinjection. To estimate the number and type of follicles per injection, 23 ovaries were batched and treated with Liberase TM, as described above, then evaluated by 14 independent hemocytometer measurements. Isolated ovarian cells were pelleted and resuspended in 200 μL with 10 μL of ovarian cell suspension used for each hemocytometer measurement. Follicles were counted and staged based upon similar criteria used for endogenous follicle staging after chemotherapy. Follicle number was estimated by multiplying the average follicle counts by 10,000 to determine follicles/mL then multiplied by 0.2 to account for the starting volume (200 μL). Follicles per ovary was determined by dividing this calculated follicle number by 23 total ovaries. Follicles per injection was estimated as the number of follicles per 7 μL injection.

In vivo follicle microinjection

The experimental design and rationale for animal use (described in IACUC Protocol #: 18103002) were reviewed and approved by the University of Pittsburgh Institutional Animal Care and Use Committee (IACUC). Eight-week old CTx female mice (NCR nu/nu) were anesthetized and placed on the operating table with their back exposed. A single midline dorsal incision (0.5 cm) was made using small scissors. Subcutaneous connective tissue was then freed from the underlying muscle on each side using blunt forceps. Once the ovary was located under the thin muscle layer, a small incision (<1 cm) was made to gain entry to the peritoneal cavity. The edge of the incision was held with tooth forceps, while the ovarian fat pad was removed to expose the ovary and surrounding bursa. A small volume (<10 μL) of chilled follicle-OECM pre-gel was transferred to a glass needle (filament Cat#: FB245B and borosilicate glass micro pipette Cat#: B100-75-10) then secured to a pressurized microinjection system. The Eppendorf microinjection system (TransferMan NK2 and

FemtoJet) was used for follicle delivery and surgical manipulation observed under a Nikon SMZ stereomicroscope. The loaded needle was positioned perpendicular to the ovary and guided into the ovarian cortex, where the follicle-OECM mixture was slowly injected at a constant pressure ranging from 50 to 250 hPa. To access the ovarian cortex, the periovarian bursa was punctured and the needle was inserted approximately 1 mm into the ovarian cortex. For each injection, approximately $1.0x10^3$ follicles were transplanted. The same surgical and injection procedures were performed contralaterally. The follicle-injected ovaries were placed back into the abdominal cavity, the muscle layers were sutured, and the skin incision was stapled.

Mating study

Two weeks after injection both the follicle recipient and non-injected control CTx nude female mice were bred with male nude mice (NCR nu/nu, Taconic). The breeding was conducted for three cycles, which concluded at 106 days, on average. Pups were fostered within 1 day, with NCR nu/+ (Taconic) females due to the lack of developed mammary glands in the nude mouse strain used for recipients. The pups were then weaned at 3–4 weeks old. Mice (DBA-GFP/nu−, Orwig Lab) inherited from the follicle injected recipients were selected based on physical traits consisting of fur, dark eyes or GFP expression. Genotyping was performed using mouse tail DNA and standard PCR with the following primers: GFP forward primer sequence (GAA CGG CAT CAA GGT GAA CT); GFP reverse primer sequence (TGC TCA GGT AGT GGT TGT CG); β-actin forward primer sequence (CGG TTC CGA TGC CCT GAG GCT CTT); β-actin reverse primer sequence (CGT CAC ACT TCA TGA TGG AAT TGA) (primers prepared by Integrated DNA Technologies, Inc.). PCR products were run on a 2.5% agarose gel and imaged under UV light. The resulting pups were grown to 8 weeks and bred for fertility status. Second generation breeding pairs consisted of a GFP/nu− experimental female and DBA/2 control male (Jackson Laboratory), a GFP/nu− experimental female and GFP/nu− experimental male, and a DBA/2 control female and GFP/nu− experimental male. Breeding pairs were separated after 2 weeks.

Immunofluorescence staining and imaging of microinjected ovaries

Ovaries were excised at the conclusion of the third breeding cycle and fixed in 4% PFA overnight then embedded in paraffin. Tissues were serial sectioned and stained with DAPI to evaluate the presence of transplanted GFP+ follicles. Four ovaries were evaluated per treatment group. A Nikon Eclipse Ti inverted microscope and NIS Elements software were used to capture representative images of GFP positive structures within each tissue section. DAPI and FITC channels were taken separately and merged to demonstrate the population of cells expressing GFP.

Statistical analysis

All data were expressed as mean ± s.e.m and plotted using GraphPad Prism 7.02. For the analysis of normally (parametrically) distributed data, the individual means were compared using an unpaired, two-tailed, t-test. For the analysis of non-parametrically distributed data, the mean ranks were compared using an unpaired, one-way ANOVA (Kruskal-Wallis) with adjusted P-values calculated based upon Dunn's multiple comparisons test. Exact P-values resulting from the statistical analysis are presented within each figure.

Acknowledgements

We would like to acknowledge funds provided from an anonymous donor and Magee-Womens Research Institute to Dr. Orwig. Also, thanks to the lab animal resource staff of Magee-Womens Research Institute. Special thanks to the Center for Biologic Imaging (CBI) at the University of Pittsburgh for their expertise and use of equipment for obtaining both SEM and multi-photon images. We also acknowledge the NIH Fellows Editorial Board for their comments and feedback on the manuscript. This research was supported in part by the Intramural Research Program of the NIH, NCI, CCR, CIL.

Author contributions

M.J.B., B.N.B and K.E.O. contributed to the study design and prepared the manuscript. M.J.B. developed the protocol for ovarian tissue decellularization, prepared OECM hydrogels, performed characterization of decellularized ovarian tissues (DNA, HYP, sGAG) and hydrogels (rheology and turbidimetric testing), isolated follicles and prepared follicle suspensions for *in vivo* studies, performed immunofluorescent staining and imaging of transplant recipient ovaries and genotyped litters. M.S. performed follicle microinjection surgeries. K.E.O, M.S. and S.R.S. designed the breeding strategy and performed all mating studies. A.I. and A.L.N. performed protein extractions and ELISAs. M.J.B., Z.X. and S.D. validated antibodies and performed IHC staining and imaging. S.D. performed SEM imaging of ovarian tissues and hydrogels. M.J.B and A.D. analyzed SEM images of OECM hydrogels to assess fiber network characteristics. Z.W.C. performed staining, imaging and follicle quantification of CTx ovaries. All authors contributed to the final editing and approval of the manuscript.

Declaration of conflicting interests

The author(s) declared no potential conflicts of interest with respect to the research, authorship, and/or publication of this article.

Funding

The author(s) received no financial support for the research, authorship, and/or publication of this article.

ORCID iD

Michael J Buckenmeyer https://orcid.org/0000-0003-2202-7215

Data availability

There are no restrictions on the data presented in this study. The data will be made available by the corresponding authors upon reasonable request.

Supplemental material

Supplemental material for this article is available online.

References

1. Bates GW and Bowling M. Physiology of the female reproductive axis. *Periodontol 2000* 2013; 61: 89–102.
2. Jones ASK and Shikanov A. Follicle development as an orchestrated signaling network in a 3D organoid. *J Biol Eng* 2019; 13: 2–2.
3. Bedoschi G, Navarro PA and Oktay K. Chemotherapy-induced damage to ovary: mechanisms and clinical impact. *Future Oncol* 2016; 12: 2333–2344.
4. Meirow D and Nugent D. The effects of radiotherapy and chemotherapy on female reproduction. *Hum Reprod Update* 2001; 7: 535–543.
5. Oktay K and Sonmezer M. Chemotherapy and amenorrhea: risks and treatment options. *Curr Opin Obstet Gynecol* 2008; 20: 408–415.
6. Filatov MA, Khramova YV, Kiseleva MV, et al. Female fertility preservation strategies: cryopreservation and ovarian tissue in vitro culture, current state of the art and future perspectives. *Zygote* 2016; 24: 635–653.
7. Paulini F, Vilela JM, Chiti MC, et al. Survival and growth of human preantral follicles after cryopreservation of ovarian tissue, follicle isolation and short-term xenografting. *Reprod Biomed Online* 2016; 33: 425–432.
8. Silber S. Ovarian tissue cryopreservation and transplantation: scientific implications. *J Assist Reprod Genet* 2016; 33: 1595–1603.
9. Xu M, Banc A, Woodruff TK, et al. Secondary follicle growth and oocyte maturation by culture in alginate hydrogel following cryopreservation of the ovary or individual follicles. *Biotechnol Bioeng* 2009; 103: 378–386.
10. Zhang H, Yang Y, Ma W, et al. The revascularization and follicular survival of mouse ovarian grafts treated with FSH during cryopreservation by vitrification. *Cryo Letters* 2016; 37: 88–102.
11. Andersen CY, Rosendahl M, Byskov AG, et al. Two successful pregnancies following autotransplantation of frozen/thawed ovarian tissue. *Hum Reprod* 2008; 23: 2266–2272.
12. Donnez J, Dolmans MM, Demylle D, et al. Livebirth after orthotopic transplantation of cryopreserved ovarian tissue. *Lancet* 2004; 364: 1405–1410.
13. Meirow D, Levron J, Eldar-Geva T, et al. Pregnancy after transplantation of cryopreserved ovarian tissue in a patient with ovarian failure after chemotherapy. *New Engl J Med* 2005; 353: 318–321.
14. Silber SJ, Lenahan KM, Levine DJ, et al. Ovarian transplantation between monozygotic twins discordant for premature ovarian failure. *New Engl J Med* 2005; 353: 58–63.
15. Xiong J, Lu Z, Wu M, et al. Intraovarian transplantation of female germline stem cells rescue ovarian function in chemotherapy-injured ovaries. *PLoS One* 2015; 10: e0139824.
16. Zhang Y, Yang Z, Yang Y, et al. Production of transgenic mice by random recombination of targeted genes in female germline stem cells. *J Mol Cell Biol* 2011; 3: 132–141.
17. Zou K, Yuan Z, Yang Z, et al. Production of offspring from a germline stem cell line derived from neonatal ovaries. *Nat Cell Biol* 2009; 11: 631–636.
18. Oatley J and Hunt PA. Of mice and (wo)men: purified oogonial stem cells from mouse and human ovaries. *Biol Reprod* 2012; 86: 196.
19. Wagner M, Yoshihara M, Douagi I, et al. Single-cell analysis of human ovarian cortex identifies distinct cell populations but no oogonial stem cells. *Nat Commun* 2020; 11: 1147.
20. Park MR, Choi YJ, Kwon DN, et al. Intraovarian transplantation of primordial follicles fails to rescue chemotherapy injured ovaries. *Sci Rep* 2013; 3: 1384.
21. Saldin LT, Cramer MC, Velankar SS, et al. Extracellular matrix hydrogels from decellularized tissues: Structure and function. *Acta Biomater* 2017; 49: 1–15.
22. Spang MT and Christman KL. Extracellular matrix hydrogel therapies: In vivo applications and development. *Acta Biomater* 2018; 68: 1–14.
23. Henning NF, LeDuc RD, Even KA, et al. Proteomic analyses of decellularized porcine ovaries identified new matrisome proteins and spatial differences across and within ovarian compartments. *Sci Rep* 2019; 9: 20001.
24. Ouni E, Vertommen D, Chiti MC, et al. A draft map of the human ovarian proteome for tissue engineering and clinical applications. *Mol Cell Proteomics* 2019; 18: S159–S173.
25. Laronda MM, Jakus AE, Whelan KA, et al. Initiation of puberty in mice following decellularized ovary transplant. *Biomaterials* 2015; 50: 20–29.
26. Jakus AE, Laronda MM, Rashedi AS, et al. "Tissue papers" from organ-specific decellularized extracellular matrices. *Adv Funct Mater* 2017; 27: 1700992.
27. Pors SE, Ramløse M, Nikiforov D, et al. Initial steps in reconstruction of the human ovary: survival of pre-antral stage follicles in a decellularized human ovarian scaffold. *Hum Reprod* 2019; 34: 1523–1535.
28. White LJ, Taylor AJ, Faulk DM, et al. The impact of detergents on the tissue decellularization process: a ToF-SIMS study. *Acta Biomater* 2017; 50: 207–219.
29. Faulk DM, Carruthers CA, Warner HJ, et al. The effect of detergents on the basement membrane complex of a biologic scaffold material. *Acta Biomater* 2014; 10: 183–193.
30. Xu H, Xu B, Yang Q, et al. Comparison of decellularization protocols for preparing a decellularized porcine annulus fibrosus scaffold. *PLoS One* 2014; 9: e86723–e86723.
31. Gratzer PF, Harrison RD and Woods T. Matrix alteration and not residual sodium dodecyl sulfate cytotoxicity affects the cellular repopulation of a decellularized matrix. *Tissue Eng* 2006; 12: 2975–2983.
32. Brown BN, Freund JM, Han L, et al. Comparison of three methods for the derivation of a biologic scaffold composed of adipose tissue extracellular matrix. *Tissue Eng Part C Methods* 2011; 17: 411–421.

33. Laronda MM, Rutz AL, Xiao S, et al. A bioprosthetic ovary created using 3D printed microporous scaffolds restores ovarian function in sterilized mice. *Nat Commun* 2017; 8: 15261.
34. Shea LD, Woodruff TK and Shikanov A. Bioengineering the ovarian follicle microenvironment. *Annu Rev Biomed Eng* 2014; 16: 29–52.
35. Crapo PM, Gilbert TW and Badylak SF. An overview of tissue and whole organ decellularization processes. *Biomaterials* 2011; 32: 3233–3243.
36. Keane TJ, Swinehart IT and Badylak SF. Methods of tissue decellularization used for preparation of biologic scaffolds and in vivo relevance. *Methods* 2015; 84: 25–34.
37. Irving-Rodgers HF and Rodgers RJ. Extracellular matrix of the developing ovarian follicle. *Semin Reprod Med* 2006; 24: 195–203.
38. Woodruff TK and Shea LD. The role of the extracellular matrix in ovarian follicle development. *Reprod Sci* 2007; 14: 6–10.
39. MacDonald JA, Takai Y, Ishihara O, et al. Extracellular matrix signaling activates differentiation of adult ovary-derived oogonial stem cells in a species-specific manner. *Fertil Steril* 2019; 111: 794–805.
40. Berkholtz CB, Lai BE, Woodruff TK, et al. Distribution of extracellular matrix proteins type I collagen, type IV collagen, fibronectin, and laminin in mouse folliculogenesis. *Histochem Cell Biol* 2006; 126: 583–592.
41. Scott JE, Carlsson IB, Bavister BD, et al. Human ovarian tissue cultures: extracellular matrix composition, coating density and tissue dimensions. *Reprod Biomed Online* 2004; 9: 287–293.
42. Gruijters MJ, Visser JA, Durlinger AL, et al. Anti-Müllerian hormone and its role in ovarian function. *Mol Cell Endocrinol* 2003; 211: 85–90.
43. Edson MA, Nagaraja AK and Matzuk MM. The mammalian ovary from genesis to revelation. *Endocr Rev* 2009; 30: 624–712.
44. Rojas J, Chávez-Castillo M, Olivar LC, et al. Physiologic course of female reproductive function: a molecular look into the prologue of Life. *J Pregnancy* 2015; 2015: 715735.
45. Brown B, Lindberg K, Reing J, et al. The basement membrane component of biologic scaffolds derived from extracellular matrix. *Tissue Eng* 2006; 12: 519–526.
46. D'Amore A, Stella JA, Wagner WR, et al. Characterization of the complete fiber network topology of planar fibrous tissues and scaffolds. *Biomaterials* 2010; 31: 5345–5354.
47. Morgan S, Anderson RA, Gourley C, et al. How do chemotherapeutic agents damage the ovary? *Hum Reprod Update* 2012; 18: 525–535.
48. Skaznik-Wikiel ME, McGuire MM, Sukhwani M, et al. Granulocyte colony-stimulating factor with or without stem cell factor extends time to premature ovarian insufficiency in female mice treated with alkylating chemotherapy. *Fertil Steril* 2013; 99: 2045–54.e3.
49. Schmidt KL, Ernst E, Byskov AG, et al. Survival of primordial follicles following prolonged transportation of ovarian tissue prior to cryopreservation. *Hum Reprod* 2003; 18: 2654–2659.
50. Kim J, Perez AS, Claflin J, et al. Synthetic hydrogel supports the function and regeneration of artificial ovarian tissue in mice. *NPJ Regen Med* 2016; 1: 16010.
51. Schmidt KL, Byskov AG, Nyboe Andersen A, et al. Density and distribution of primordial follicles in single pieces of cortex from 21 patients and in individual pieces of cortex from three entire human ovaries. *Hum Reprod* 2003; 18: 1158–1164.
52. Hornstein MD. State of the ART: assisted reproductive technologies in the United States. *Reproductive Sciences* 2016; 23: 1630–1633.
53. Huang JYJ and Rosenwaks Z. Assisted reproductive techniques. *Methods Mol Biol* 2014; 1154: 171–231.
54. Jeruss JS and Woodruff TK. Preservation of fertility in patients with cancer. *New Engl J Med* 2009; 360: 902–911.
55. Kim SY, Kim SK, Lee JR, et al. Toward precision medicine for preserving fertility in cancer patients: existing and emerging fertility preservation options for women. *J Gynecol Oncol* 2016; 27: e22.
56. Rodriguez-Macias Wallberg KA, Keros V and Hovatta O. Clinical aspects of fertility preservation in female patients. *Pediatr Blood Cancer* 2009; 53: 254–260.
57. Donnez J and Dolmans MM. Transplantation of ovarian tissue. *Best Pract Res Clin Obstet Gynaecol* 2014; 28: 1188–1197.
58. Grynberg M, Poulain M, Sebag-Peyrelevade S, et al. Ovarian tissue and follicle transplantation as an option for fertility preservation. *Fertil Steril* 2012; 97: 1260–1268.
59. Salama M and Woodruff TK. New advances in ovarian autotransplantation to restore fertility in cancer patients. *Cancer Metastasis Rev* 2015; 34: 807–822.
60. Smitz J, Dolmans MM, Donnez J, et al. Current achievements and future research directions in ovarian tissue culture, in vitro follicle development and transplantation: implications for fertility preservation. *Hum Reprod Update* 2010; 16: 395–414.
61. Fabbri R, Macciocca M, Vicenti R, et al. First Italian birth after cryopreserved ovarian tissue transplantation in a patient affected by non-Hodgkin's lymphoma. *Int J Hematol Oncol* 2018; 7: IJH08.
62. Fabbri R, Seracchioli R, Vicenti R, et al. Successful achievement after heterotopic transplantations of long-term stored ovarian tissue in Hodgkin's lymphoma survivor. *Gynecol Endocrinol* 2019; 35: 470–472.
63. Khattak H, Malhas R, Craciunas L, et al. Correction to: Fresh and cryopreserved ovarian tissue transplantation for preserving reproductive and endocrine function: a systematic review and individual patient data meta-analysis. *Hum Reprod Update* 2022; 28: 455–416.
64. Telfer EE. Future developments: in vitro growth (IVG) of human ovarian follicles. *Acta Obstet Gynecol Scand* 2019; 98: 653–658.
65. Batchvarov IS, Taylor RW, Bustamante-Marín X, et al. A grafted ovarian fragment rescues host fertility after chemotherapy. *Mol Hum Reprod* 2016; 22: 842–851.
66. Rios PD, Kniazeva E, Lee HC, et al. Retrievable hydrogels for ovarian follicle transplantation and oocyte collection. *Biotechnol Bioeng* 2018; 115: 2075–2086.
67. Hassanpour A, Talaei-Khozani T, Kargar-Abarghouei E, et al. Decellularized human ovarian scaffold based on a sodium lauryl ester sulfate (SLES)-treated protocol, as a natural three-dimensional scaffold for construction of bioengineered ovaries. *Stem Cell Res Ther* 2018; 9: 252.
68. Kniazeva E, Hardy AN, Boukaidi SA, et al. Primordial follicle transplantation within designer biomaterial grafts produce live births in a mouse infertility model. *Sci Rep* 2015; 5: 17709.

69. Smith RM, Shikanov A, Kniazeva E, et al. Fibrin-mediated delivery of an ovarian follicle pool in a mouse model of infertility. *Tissue Eng Part A* 2014; 20: 3021–3030.
70. Luyckx V, Dolmans MM, Vanacker J, et al. A new step toward the artificial ovary: survival and proliferation of isolated murine follicles after autologous transplantation in a fibrin scaffold. *Fertil Steril* 2014; 101: 1149–1156.
71. Shikanov A, Zhang Z, Xu M, et al. Fibrin encapsulation and vascular endothelial growth factor delivery promotes ovarian graft survival in mice. *Tissue Eng Part A* 2011; 17: 3095–3104.
72. Desai N, Alex A, AbdelHafez F, et al. Three-dimensional in vitro follicle growth: overview of culture models, biomaterials, design parameters and future directions. *Reprod Biol Endocrinol* 2010; 8: 119.
73. Amorim CA, Van Langendonckt A, David A, et al. Survival of human pre-antral follicles after cryopreservation of ovarian tissue, follicular isolation and in vitro culture in a calcium alginate matrix. *Hum Reprod* 2008; 24: 92–99.
74. Laronda MM, Duncan FE, Hornick JE, et al. Alginate encapsulation supports the growth and differentiation of human primordial follicles within ovarian cortical tissue. *J Assist Reprod Genet* 2014; 31: 1013–1028.
75. Tagler D, Makanji Y, Anderson NR, et al. Supplemented αMEM/F12-based medium enables the survival and growth of primary ovarian follicles encapsulated in alginate hydrogels. *Biotechnol Bioeng* 2013; 110: 3258–3268.
76. Tagler D, Makanji Y, Tu T, et al. Promoting extracellular matrix remodeling via ascorbic acid enhances the survival of primary ovarian follicles encapsulated in alginate hydrogels. *Biotechnol Bioeng* 2014; 111: 1417–1429.
77. Xu M, Barrett SL, West-Farrell E, et al. In vitro grown human ovarian follicles from cancer patients support oocyte growth. *Hum Reprod* 2009; 24: 2531–2540.
78. Xu M, Kreeger PK, Shea LD, et al. Tissue-engineered follicles produce live, fertile offspring. *Tissue Eng* 2006; 12: 2739–2746.
79. Xu M, West-Farrell ER, Stouffer RL, et al. Encapsulated three-dimensional culture supports development of nonhuman primate secondary follicles. *Biol Reprod* 2009; 81: 587–594.
80. Xu J, Lawson MS, Yeoman RR, et al. Fibrin promotes development and function of macaque primary follicles during encapsulated three-dimensional culture. *Hum Reprod* 2013; 28: 2187–2200.
81. Shikanov A, Xu M, Woodruff TK, et al. Interpenetrating fibrin-alginate matrices for in vitro ovarian follicle development. *Biomaterials* 2009; 30: 5476–5485.
82. Ahn JI, Kim GA, Kwon HS, et al. Culture of preantral follicles in poly(ethylene) glycol-based, three-dimensional hydrogel: a relationship between swelling ratio and follicular developments. *J Tissue Eng Regen Med* 2015; 9: 319–323.
83. Shikanov A, Smith RM, Xu M, et al. Hydrogel network design using multifunctional macromers to coordinate tissue maturation in ovarian follicle culture. *Biomaterials* 2011; 32: 2524–2531.
84. McLaughlin M, Albertini DF, Wallace WHB, et al. Metaphase II oocytes from human unilaminar follicles grown in a multistep culture system. *Mol Hum Reprod* 2018; 24: 135–142.
85. Mouloungui E, Zver T, Roux C, et al. A protocol to isolate and qualify purified human preantral follicles in cases of acute leukemia, for future clinical applications. *J Ovarian Res* 2018; 11: 4–4.
86. Freytes DO, Martin J, Velankar SS, et al. Preparation and rheological characterization of a gel form of the porcine urinary bladder matrix. *Biomaterials* 2008; 29: 1630–1637.
87. Gelman RA, Williams BR and Piez KA. Collagen fibril formation. Evidence for a multistep process. *J Biol Chem* 1979; 254: 180–186.